Journal of Molecular Liquids 224 (2016) 480–491

Contents lists available at ScienceDirect

Journal of Molecular Liquids

journal homepage: www.elsevier.com/locate/molliq

Synthesis and study of ionic interactions by volumetric, transport, FT-IR and computational methods of alkyl imidazolium acetate ionic liquid with molecular solvents (DMSO, DMF & EG) at T = (293.15–363.15) K

Venkatramana Losetty [a,*], Cecilia Devi Wilfred [a,b], M. Chandra Shekar [c]

[a] Center of Research in Ionic Liquids (CORIL), Universiti Teknologi PETRONAS, Bandar Seri Iskandar, Perak 32610, Malaysia
[b] Faculty of Fundamental and Applied Science, Universiti Teknologi PETRONAS, 32610 Tronoh, Perak, Malaysia
[c] Department of Physics, Vignan Institute of Technology and Science, Deshmukhi 508284, Telangana, India

ARTICLE INFO

Article history:
Received 3 September 2016
Received in revised form 4 October 2016
Accepted 10 October 2016
Available online 11 October 2016

Keywords:
Apparent molar expansibility
Redlich-Mayer equation
Jones-Dole equation
Density functional theory (DFT)
FT-IR study

ABSTRACT

In this work, the ionic liquid (IL) 1-octyl-3-methylimidazolium acetate [C_1C_8IM][OAc] was synthesized through the neutralization process followed by metathesis method. The experimental density (ρ) and viscosity (η) of the pure components as well as binary solutions of IL with molecular solvents such as dimethyl sulfoxide (DMSO), dimethylformamide (DMF) and ethylene glycol (EG) have been measured as a function of concentration of IL in terms of molality at T = (293.15–363.15) K and at 0.1 Mpa pressure. From the experimental density data apparent molar volumes (V_Φ), apparent molar volumes at infinity dilution (V_Φ^∞), apparent molar limiting parameter (S_v) and apparent molar expansibility (E_Φ^0) were calculated with the help of Redlich-Mayer equation. The experimental viscosity data was analyzed by using the Jones-Dole equation to evaluate the empirical coefficients (A and B). The obtained parameters were analyzed to understand the ion-solvent or ion-ion interactions of studied binary solutions at various temperature ranges. In addition, FT-IR spectroscopy study was performed to justify the hydrogen bonding interactions. Density functional theory (DFT) was performed to understand the intra-ionic and inter-ionic interactions between the IL and molecular solvents. The subsequent FT-IR and computational results were good agreement with experimental data.

1. Introduction

Room temperature ionic liquids (RTILs) are new class of molten salts, which have been received significant attention due to their exclusive physico-chemical properties such as low melting temperature, large liquidus range, negligible vapor pressure, non-flammability, high thermal stability, complex behavior as solvents and catalyst for organic synthesis [1,2]. The physico-chemical properties of the ILs can be changed due to the appropriate selection of cation and/or anion [3]. One class of salts, acetate based ILs (AcILs) are improved hydrogen bonding acceptor ability, which have been widely used as promising solvents for CO_2 absorption and cellulose and or biomass dissolution. Acetate based ILs are able to strongly bonded with CO_2 and hydrogen bond donor groups (-OH group). An industrial and academic communities have been significantly attracting the acetate based ILs because of a new generation "green ionic liquids". AcILs have high solubility nature, good catalytic abilities, hence which are widely used in "enzyme-friendly" co-solvents for resolution of amino acids and some catalytic reactions [4]. Nevertheless, most of the researchers focused on acetate based ILs because of exhibiting low toxicity, low corrosive, favorable biodegradability and also poorly investigated their thermophysical properties [5]. To better understand the nature of the molten salts and wisely developing their applications, information about the thermodynamic and thermophysical properties of ILs and their mixtures with molecular solvents are essential. In binary systems, the contribution of thermophysical properties is sensitive to the entire range of interactions such as solute-solvent, solute-solute and solute-co-solvent. Till date, a number of researchers have reported the thermophysical properties of ILs and their solutions with molecular solvents such as density, viscosity, conductivity, heat capacity, enthalpy, surface tension, refractive index *etc.* [6,7]. However, few researchers have focused on the limiting molar quantities which are obtained from the dilute solution regions such as apparent molar volumes, apparent molar volumes at infinity dilution and limiting apparent molar expansibilities, which are important for the investigation of interactions between ILs and molecular solvents and design of process engineering [8]. Knowledge of the viscosity of an electrolyte solution is essential for the design of numerous industrial processes and it provides useful information about solutions geometry and interactions [9].

In this work, the molecular solvents such as dimethyl sulfoxide (DMSO), dimethylformamide (DMF) and ethylene glycol (EG) were chosen because those of their wide range of applications. The polar

* Corresponding author.
E-mail address: ramanapvkn@gmail.com (V. Losetty).

http://dx.doi.org/10.1016/j.molliq.2016.10.046
0167-7322/

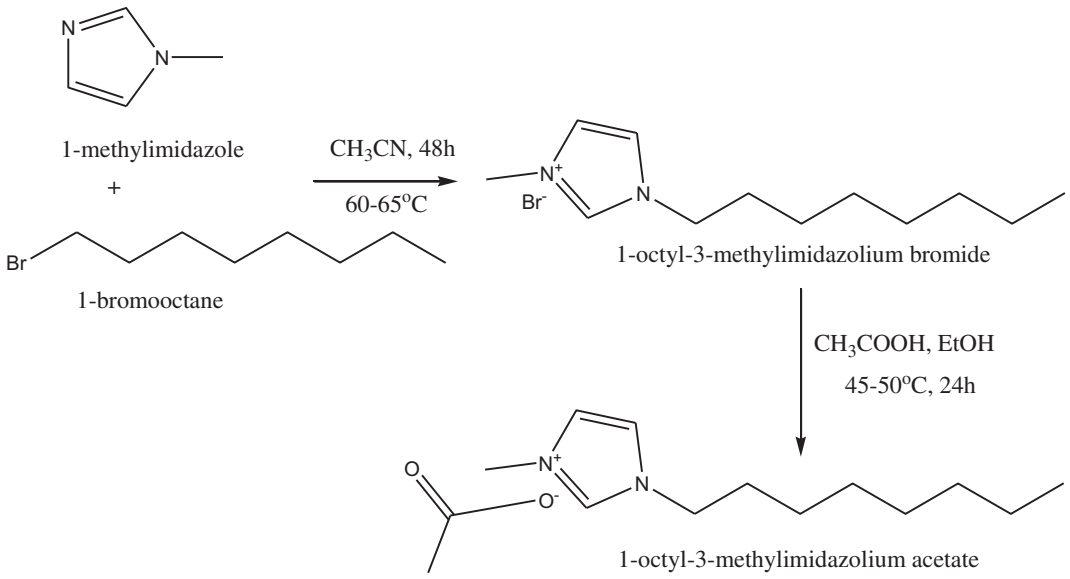

Scheme 1. Two pot synthesis of 1-octyl-3-methylimidazolium acetate.

Table 1
Literature comparison of an experimentally measured density (ρ) and viscosity (η) of pure [C_1C_8IM][OAc], DMSO, DMF and EG at T = (293.15 to 363.15) K.

T/K	[C_1C_8IM][OAc]*		DMSO				DMF				EG			
	$\rho \times 10^{-3}$/kg·m^{-3}	η/mPa·s	$\rho \times 10^{-3}$/kg·m^{-3}		η/mPa·s		$\rho \times 10^{-3}$/kg·m^{-3}		η/mPa·s		$\rho \times 10^{-3}$/kg·m^{-3}		η/mPa·s	
			Exp.	Lit.	Exp.	Lit.	Exp.	Lit.	Exp.	Lit.	Exp.	Lit.	Exp.	Lit.
293.15	1.1548	420.86	1.1000	1.10076[a] 1.10086[c]	2.368	2.244[g] 2.213[h]	0.9489	0.94939[f]	0.981	0.864[f]	1.1130	1.1137[i]	21.225	20.833[i]
303.15	1.1474	217.20	1.0898	1.09073[a] 1.09073[b] 1.09081[c] 1.09037[d]	1.937	1.843[b] 1.786[d]	0.9391	0.94009[d] 0.93945[e] 0.93983[f]	0.871	0.759[d] 0.760[e] 0.766[f]	1.1058	1.1032[i]	14.019	13.646[i]
313.15	1.1405	122.39	1.0798	1.08069[a] 1.08069[b] 1.08077[c] 1.08058[d]	1.650	1.556[b] 1.506[d]	0.9295	0.93074[d] 0.92986[e] 0.93027[f]	0.747	0.678[d] 0.675[e] 0.684[f]	1.0988	1.0936[i] 1.0983[j] 1.0936[k]	9.696	9.443[i] 9.444[j] 9.443[k]
323.15	1.1335	74.24	1.0698	1.07066[a] 1.07066[b] 1.07073[c] 1.07075[d]	1.385	1.337[b] 1.278[d]	0.9199	0.92125d 0.92092e 0.92071[f]	0.705	0.608[d] 0.608[e] 0.617[f]	1.0915	1.0847[i] 1.09116[j] 1.09116[k]	7.021	6.992[i] 6.794[j] 6.992[k]
333.15	1.1266	48.01	1.0596	1.06063[a] 1.06063[b] 1.06068[c] 1.06026[d]	1.202	1.165[b] 1.104[d]	0.9102	0.91117[d] 0.91064[e] 0.91113[f]	0.643	0.552[d] 0.552[e] 0.559[f]	1.0843	1.0764[i] 1.08394[j] 1.0764[k]	5.254	5.060[i] 5.065[j] 5.06[k]
343.15	1.1196	32.72	1.0497	1.05058[a] 1.05058[b] 1.05062[c] 1.05030[d]	1.052	1.028[b] 0.962[d]	0.9003	0.90154[d] 0.90172[e] 0.90151[f]	0.590	0.501[d] 0.502[e] 0.510[f]	1.0769	1.0675[i] 1.07453[j] 1.0676[k]	4.060	3.987[i] 3.879[j] 3.987[k]
353.15	1.1127	23.31	1.0395	1.04051[a] 1.04051[b] 1.04054[c] 1.04003[d]	0.934	0.917[b] 0.850[d]	0.8905	0.89154[d] 0.89144[e] 0.89186[f]	0.544	0.459[d] 0.460[e] 0.470[f]	1.0694	1.0600[i] 1.06972[j] 1.0600[k]	3.208	3.021[i] 3.058[j] 3.021[k]
363.15	1.1061	17.25	1.0297	–	0.832	–	0.8807	–	0.503	–	1.0619	–	2.583	–

* From the ^{1}H NMR spectroscopic technique, the purity of synthesized ionic liquid is estimated to be 98.7%.
Standard uncertainties are $u(\rho) = 0.5$ kg·m^{-3}, $u(\eta) = 1\%$, $u(P) = 2$ kPa and $u(T) = 0.02$ K. The standard uncertainties for density and viscosity include the effect of water impurity identified in Table S3 and Fig. S11 of the Supporting information. No extrapolation of the reported property values to zero water content was done.

[a] Ref [13].
[b] Ref [14].
[c] Ref [15].
[d] Ref [16].
[e] Ref [17].
[f] Ref [18].
[g] Ref [19].
[h] Ref [20].
[i] Ref [21].
[j] Ref [22].
[k] Ref [23].

aprotic solvent dimethyl sulfoxide (DMSO) has a very low toxicity and it acts as cryoprotective agent. Similarly, *N,N*-dimethylformamide (DMF) as an organic solvent has been employed in fertilizers and pharmaceutical chemistry due to their distinctive properties [10]. EG also has similar characteristic of alcohols and undergoes reactions typically as of alcohols and diols. It has a low melting point, thus being an alcohol, it is widely used as an automotive engine antifreeze [11].

In the present investigation 1-octyl-3-methylimidazolium acetate was synthesized. The density and viscosity of pure compounds as well as binary mixtures of IL with DMSO, DMF and EG as function of IL concentration in terms of molality at T = (293.15–363.15) K at ambient pressure were measured. A detailed and systematic measurement of thermophysical properties of IL mixtures is essentially required to gain their novel application in basic research. So, the measured density and viscosity can be useful to determine the ionic interactions such as solute-solute or solute-solvent interactions by fitting to Redlich-Mayer and Jones-Dole equations respectively. FT-IR spectroscopy study was performed to explain the solute-solvent interactions through the hydrogen bonding. In addition, density functional theory (DFT) was performed to understand the ionic interactions between the ions of IL and organic solvents. To our best knowledge there is no literature available regarding the synthesis of $[C_1C_8IM][OAc]$ ionic liquid, measurements and determinations of above said thermophysical properties, besides that elucidation of ionic interactions by FT-IR spectroscopy and density functional theory.

2. Materials and methods

2.1. Materials

The ionic liquid was synthesized and further study has been carried out by using analytical grade starting materials without further purifications. These are: 1-methylimidazole (Aldrich, 99%), 1-bromooctane (Aldrich, 99%), Acetonitrile (Aldrich, 99%), ethyl acetate (Merck, 99%), Ethanol (Merck, 99%), Glacial acetic acid (Merck, 99%) diethyl ether (Merck, 99%), dimethyl sulfoxide (Aldrich, 99%), dimethylformamide (Aldrich, 99%) and ethylene glycol (Aldrich, 99%).

2.2. Synthesis of $[C_1C_8IM][OAc]$

Two stage process is involved for the synthesis of $[C_1C_8IM][OAc]$ ionic liquid. 0.15 mol of 1-methylimidazole was charged into a three necked round bottom flask with acetonitrile as a solvent. 0.155 mol of 1-bromooctane was added and the temperature brought to 60–65 °C for 48 h with constant stirring. The obtained product is purified by 20 mL of ethyl acetate (20 mL × 3), and the trace of ethyl acetate was removed by using the vacuum rotary at 70 °C. The resultant pale yellowish, highly viscous 1-octyl-3-methylimidazolium bromide was taken in to a round bottomed flask which has ethanol solvent. An equimolar quantity of glacial acetic acid was added drop wise at 5–10 °C for 30 min and then the temperature was raised to 45–50 °C for 24 h. The excess amount of acetic acid and unreacted starting material were removed by the purification process with diethyl ether (20 mL × 3). The obtained low viscus, colorless liquid was dried at 65–70 °C at high vacuum for 24 h [5,12]. The IL was characterized by ^1H and ^{13}C NMR spectroscopy techniques, and the purity was estimated to be 98.7%. The schematic representation of the synthesis of $[C_1C_8IM][OAc]$ given as Scheme 1.

2.3. Characterization of $[C_1C_8IM][OAc]$

^1H and ^{13}C spectrums were recorded by Bruker Avance 500 spectrometer, which are given in Figs. S1–S3.

Table 2
Molality (m) and density (ρ) of $[C_1C_8IM][OAc]$ Ionic Liquid with DMSO, DMF and EG at T = (293.15 to 363.15) K.

m/mol·kg^{-1}	293.15 K	303.15 K	313.15 K	323.15 K	333.15 K	343.15 K	353.15 K	363.15 K
ρ/kg·m^{-3} of $[C_1C_8IM][OAc]$ + DMSO								
0.0458	1101.7	1092.6	1081.5	1071.2	1061.2	1051.2	1041.0	1028.9
0.0989	1102.4	1092.1	1082.1	1072.2	1062.3	1052.2	1042.3	1032.6
0.1423	1103.2	1093.1	1082.8	1073.6	1063.2	1053.5	1043.1	1033.9
0.1830	1103.9	1093.9	1084.1	1074.2	1064.2	1054.4	1044.5	1034.8
0.2315	1105.0	1095.5	1085.3	1076.0	1065.8	1055.5	1045.9	1036.3
0.2782	1105.7	1095.7	1085.9	1076.1	1066.4	1056.5	1046.7	1037.0
0.3236	1106.3	1097.1	1086.7	1077.5	1067.2	1056.8	1048.4	1038.8
0.3659	1107.2	1096.9	1087.2	1077.6	1067.9	1058.1	1048.4	1038.9
0.4115	1107.8	1098.0	1087.9	1078.8	1068.7	1059.1	1049.6	1041.4
0.4580	1108.5	1098.7	1089.0	1079.4	1069.7	1060.1	1050.4	1041.8
ρ/kg·m^{-3} of $[C_1C_8IM][OAc]$ + DMF								
0.0493	951.8	942.1	932.5	922.9	913.2	903.5	893.8	883.9
0.0919	954.1	944.5	934.9	925.4	915.8	906.1	896.3	886.6
0.1364	956.8	946.2	937.3	927.7	918.5	908.5	899.0	889.1
0.1851	958.9	949.4	940.1	930.7	921.1	911.4	901.7	891.8
0.2272	961.3	951.3	941.5	932.3	922.6	913.6	904.7	894.8
0.2776	963.1	953.6	944.2	934.7	925.2	915.7	906.1	896.4
0.3171	965.4	955.9	946.9	936.1	927.4	918.6	909.0	899.3
0.3669	967.9	958.4	949.1	939.7	930.3	920.7	911.2	901.6
0.4086	969.8	960.7	951.7	941.9	932.5	923.6	914.1	904.5
0.4578	971.8	962.5	953.2	943.8	934.4	925.0	915.6	906.2
ρ/kg·m^{-3} of $[C_1C_8IM][OAc]$ + EG								
0.0496	1113.6	1106.3	1099.2	1092.1	1084.8	1077.4	1069.9	1062.4
0.0975	1113.9	1106.7	1099.6	1092.4	1085.1	1077.8	1070.3	1062.7
0.1366	1114.1	1106.9	1099.9	1092.7	1085.5	1078.1	1070.6	1063.1
0.1841	1114.5	1107.4	1100.2	1093.0	1085.9	1078.4	1070.9	1063.4
0.2313	1114.8	1107.7	1100.5	1093.4	1086.3	1078.9	1071.3	1063.8
0.2755	1115.1	1108.0	1100.9	1093.7	1086.4	1079.1	1071.6	1064.1
0.3198	1115.4	1108.3	1101.1	1093.9	1086.7	1079.5	1071.9	1064.5
0.3698	1115.6	1108.6	1101.4	1094.1	1086.9	1079.6	1072.1	1064.6
0.4079	1115.9	1108.7	1101.8	1094.4	1087.1	1079.8	1072.4	1064.8
0.4561	1116.2	1109.0	1101.9	1094.7	1087.4	1080.0	1072.5	1064.9

Standard uncertainties are $u(m) = 5 \times 10^{-3}$ mol·kg^{-1}, $u(\rho) = 0.5$ kg·m^{-3}, $u(P) = 2$ kPa and $u(T) = 0.02$ K.

NMR ($CDCl_3$, δ ppm) ^{1}H NMR: [C1C8IM][Br]: 0.81 (t, 3H), 1.19–1.28 (m, 10H), 1.84 (t, 2H), 4.08 (s, 3H), 4.28 (t, 2H), 7.45 (d, 2H), 7.63 (d, 2H) and 10.25 (s, 1H).

[C_1C_8IM][OAc]: ^{1}H NMR: 0.81 (t, 3H), 1.19–1.27 (m, 10H), 1.85 (t, 2H), 2.01 (s, 3H), 4.05 (s, 3H), 4.26 (t, 2H), 7.43 (d, 2H), 7.58 (d, 2H) and 10.03 (s, 1H).

^{13}C NMR: 14.1, 21.0, 22.5, 26.2, 28.5, 30.2, 31.6, 36.7, 50.1, 122.0, 123.8, 137.1, 174.7.

3. Experimental methods

The water content of the synthesized IL and pure solvents were measured by Karl Fischer Titrator (Mettler Toledo DL39), the measured water content is 574 ppm for IL and about 0.02% for organic solvents. Prior to determination of the water content of the samples, the instrument was calibrated with Millipore water.

Sartorius (MSU225S-100-ID) analytical balance with ±0.01 mg accuracy was used to determine the mass of the solute and solvents individually. The binary solutions were prepared by using an air-tight stoppered glass vials to avoid the atmospheric moisture. The mixture was exposed to sonication for 3 min to make homogeneous solution.

Density and viscosity measurements of the neat IL and their binary solutions were performed at the temperature of T = (293.15–363.15) K and 0.1 MPa pressure by using an SVM3000 Anton Paar rotational Stabinger density-viscometer. The instrument is calibrated with standard ionic liquids, Millipore water followed by dry air as per supplier's instructions. The standard uncertainty of the instrument is $u(T) = \pm 0.01$ K, $u(\eta) = \pm 0.32\%$, and $u(\rho) = \pm 5 \times 10^{-4}$ g·cm^{-3} for temperature, viscosity and density respectively. The relative standard uncertainty for density and viscosity was calculated by the ratio of the standard deviation and measured data of each sample. The claimed experimental uncertainties are $u(\rho) = 0.5$ kg·m^{-3}, $u(\eta) = 1\%$, $u(P) = 2$ kPa and $u(T) = 0.02$ K. The measured density and viscosity data of pure IL and pure molecular solvents are reported in Table 1, which are in good agreement with literature data [13–23].

The solute-solvent interactions were studied by using FT-IR spectrometer (Thermoscientific, NICOLET is10 model). The optimized geometry, harmonic vibrational wave numbers and bond characteristics of the pure and hydrogen bonded complexes (binary solutions), interaction energy and natural bonding orbital (NBO) analysis have been calculated theoretically from the density functional theory (DFT-B3LYP) [24] methods with 6-31 + G and 6-311 + G basis sets. All the calculations have been carried out using the Gaussian 09 computational package [25].

4. Results and discussion

4.1. Volumetric properties

The density of the pure liquids and their mixtures have been measured as a function of IL concentration (m, 0.0451–0.4960 mol·kg^{-1}) at the temperature of T = (293.15–363.15) K at 0.1 MPa pressure. The experimental density data of IL with DMSO, DMF and EG are represented in Table 2, graphically illustrated in Figs. S4–S6. As can be observed from Table 2, the measured density of binary solutions linearly decreased with increases the temperature as well as increased with increases the IL concentration. The order of the density of the IL with molecular solvents as follows

IL + EG > IL + DMSO > IL + DMF.

Table 3
Molality (m) and apparent molar volumes (V_Φ) of [C_1C_8IM][OAc] Ionic Liquid with DMSO, DMF and EG at T = (293.15 to 363.15) K.

m/mol·kg^{-1}	293.15 K	303.15 K	313.15 K	323.15 K	333.15 K	343.15 K	353.15 K	
$V_\Phi \cdot 10^6$ m^3·mol^{-1} of [C_1C_8IM][OAc] + DMSO								
0.0458	249.77	251.82	254.43	256.88	259.30	261.77	264.33	267.48
0.0989	249.61	251.97	254.30	256.65	259.04	261.52	264.01	266.48
0.1423	249.44	251.73	254.14	256.32	258.82	261.21	263.81	266.16
0.1830	249.28	251.56	253.83	256.17	258.58	260.98	263.45	265.92
0.2315	249.04	251.19	253.55	255.74	258.20	260.70	263.09	265.54
0.2782	248.88	251.15	253.41	255.72	258.04	260.46	262.90	265.36
0.3236	248.74	250.83	253.24	255.38	257.85	260.39	262.46	264.90
0.3659	248.55	250.87	253.11	255.36	257.68	260.07	262.47	264.87
0.4115	248.40	250.62	252.95	255.07	257.49	259.82	262.17	264.22
0.4580	248.25	250.46	252.69	254.94	257.25	259.58	261.97	264.13
$V_\Phi \cdot 10^6$ m^3·mol^{-1} of [C_1C_8IM][OAc] + DMF								
0.0493	289.07	292.04	295.05	298.12	301.28	304.51	307.81	311.26
0.0919	288.38	291.30	294.30	297.31	300.43	303.64	306.96	310.32
0.1364	287.58	290.80	293.53	296.57	299.56	302.86	306.04	309.46
0.1851	286.94	289.80	292.67	295.62	298.70	301.88	305.13	308.51
0.2272	286.21	289.24	292.24	295.12	298.21	301.14	304.12	307.49
0.2776	285.69	288.53	291.40	294.36	297.39	300.47	303.65	306.93
0.3171	284.99	287.84	290.56	293.91	296.69	299.52	302.68	305.93
0.3669	284.27	287.09	289.90	292.80	295.75	298.84	301.95	305.16
0.4086	283.72	286.39	289.12	292.12	295.06	297.89	300.99	304.18
0.4578	283.13	285.87	288.65	291.53	294.46	297.45	300.50	303.62
$V_\Phi \cdot 10^6$ m^3·mol^{-1} of [C_1C_8IM][OAc] + EG								
0.0496	247.12	248.75	250.36	251.98	253.68	255.42	257.21	259.03
0.0975	247.05	248.66	250.27	251.91	253.61	255.33	257.12	258.96
0.1366	247.00	248.62	250.21	251.86	253.53	255.25	257.03	258.86
0.1841	246.92	248.51	250.13	251.78	253.43	255.19	256.97	258.79
0.2313	246.85	248.44	250.06	251.69	253.34	255.07	256.88	258.69
0.2755	246.79	248.37	249.97	251.63	253.31	255.02	256.81	258.62
0.3198	246.73	248.31	249.92	251.58	253.25	254.94	256.74	258.52
0.3698	246.68	248.25	249.85	251.53	253.20	254.91	256.68	258.49
0.4079	246.62	248.21	249.78	251.45	253.16	254.85	256.61	258.44
0.4561	246.55	248.15	249.74	251.39	253.07	254.81	256.59	258.42

Standard uncertainties are $u(m) = 5 \times 10^{-3}$ mol·kg^{-1}, $u(V_\Phi) = 0.1 \times 10^6$ m^3·mol^{-1}, $u(P) = 2$ kPa and $u(T) = 0.02$ K.

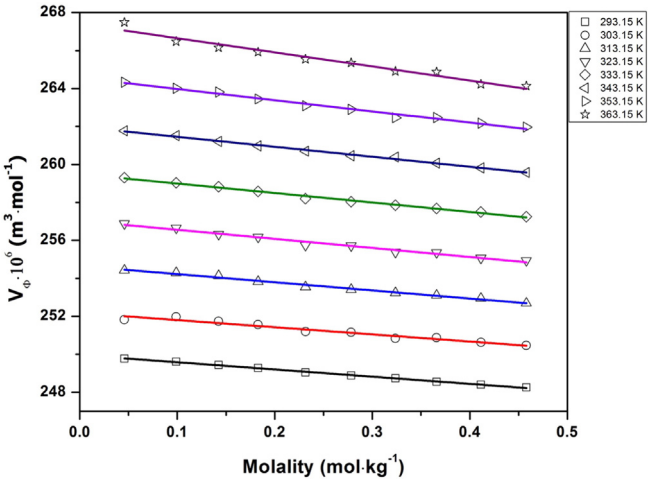

Fig. 1. Apparent molar volumes (V_Φ) of [C_1C_8IM][OAc] + DMSO as a function IL concentration.

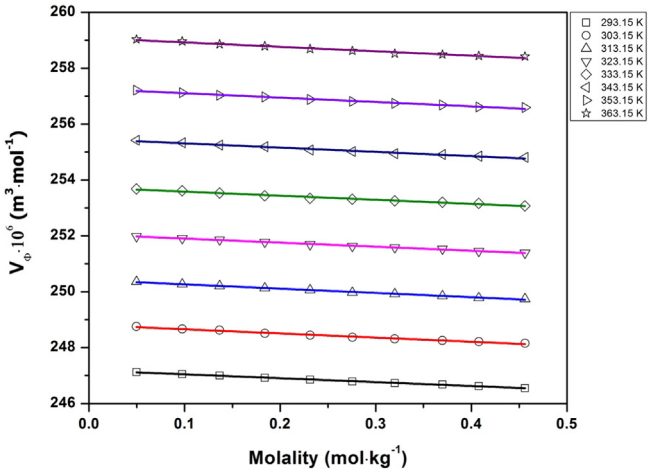

Fig. 3. Apparent molar volumes (V_Φ) of [C_1C_8IM][OAc] + EG as a function IL concentration.

Usually, apparent molar volume is defined as the volume difference between the solution and solvent per mole of solute, which is represented as follows

$$V_\Phi = \frac{\left(V - n_1 V_1^0\right)}{n_2} \tag{1}$$

where 'V' is volume of the solution V_1^0 is molar volume of the solvent, n_1 and n_2 are the number of moles of solvent and solute respectively.

The apparent molar volumes (V_Φ) of [C_1C_8IM][OAc] with studied molecular solvents were calculated from the experimental densities of the mixtures as given below

$$V_\Phi = \left[\frac{M}{\rho}\right] - \left[\frac{\rho - \rho_o}{m\rho\rho_o}\right] \tag{2}$$

where, 'M' is molar mass of IL, 'm' is molality of the IL with studied solvents, ρ and ρ_o are density of solution and solvent respectively. The calculated apparent molar volume's data at different temperatures are presented in Table 3 and graphically depicted in Figs. 1–3. From Table 3, the apparent molar volumes of investigated systems are observed to be decreasing gradually with increase of IL concentration and also linearly increased with increases of temperature. A similar behavior was reported for the systems of IL + DMSO [8], IL + DMF [26]. To describe the molality dependent apparent molar volumes, Redlich-Mayer [27] empirical equation has been used, Redlich-Mayer equation can be given by Eq. (3)

$$V_\Phi = V_\Phi^\infty + A_v m^{\frac{1}{2}} + B_v m \tag{3}$$

where V_Φ^∞ is the apparent molar volumes at infinity dilution, 'A_v' is limiting slope, which has governed by the volumetric and dielectric properties of molecular solvents. The term B_v is an empirical constant obtained by the apparent molar volume's data fitted in Eq. (3). The limiting apparent molar volume or apparent molar volume at infinity dilution (V_Φ^∞) gives the degree of solute-solvent interactions, which are effected by solvent relative permittivity, ions size and charge, pressure and temperature [28,29]. From Eq. (3), the obtained apparent molar volumes at infinity dilutionV_Φ^∞, limiting slope A_v and relative standard deviation values are listed in Table S1. The V_Φ^∞ data for all systems at wide range of temperatures are large and positive, it can be concluded that strong solute-solvent interactions occurred at infinity dilution. As seen from Table S1, it can be deduced that the magnitude of A_v is negative for all solvents with ionic liquid at all temperature ranges, which can be

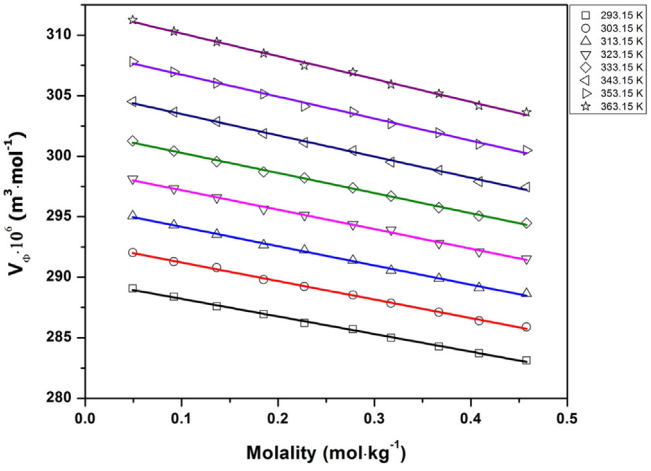

Fig. 2. Apparent molar volumes (V_Φ) of [C_1C_8IM][OAc] + DMF as a function IL concentration.

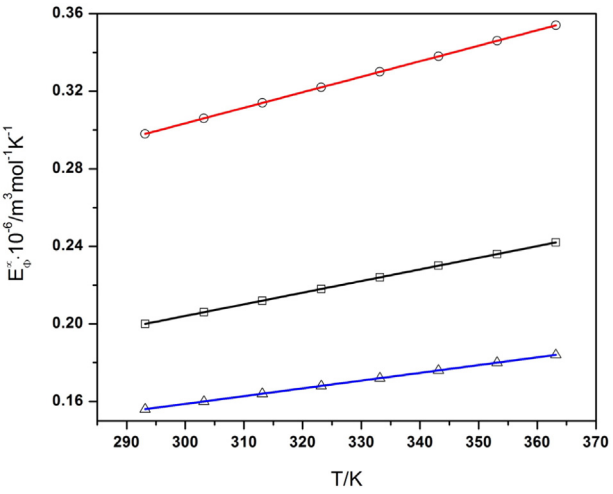

Fig. 4. Apparent molar expansibility (E_Φ^o) of [C_1C_8IM][OAc] + DMSO (□); [C_1C_8IM][OAc] + DMF (○) and [C_1C_8IM][OAc] + EG (Δ) as a function of temperature.

Table 4
Molality (m) and viscosity (η) of [C_1C_8IM][OAc] Ionic Liquid with DMSO, DMF and EG at T = (293.15 to 363.15) K.

m/mol·kg^{-1}	293.15 K	303.15 K	313.15 K	323.15 K	333.15 K	343.15 K	353.15 K	363.15 K
η mPa·s of [C_1C_8IM][OAc] + DMSO								
0.0458	2.441	1.997	1.698	1.421	1.232	1.080	0.957	0.853
0.0989	2.536	2.069	1.757	1.467	1.268	1.110	0.981	0.873
0.1423	2.598	2.127	1.815	1.498	1.302	1.129	0.999	0.890
0.1830	2.692	2.195	1.852	1.539	1.329	1.160	1.023	0.909
0.2315	2.776	2.263	1.887	1.568	1.355	1.181	1.042	0.927
0.2782	2.866	2.324	1.938	1.620	1.386	1.211	1.064	0.947
0.3236	2.986	2.408	1.997	1.672	1.428	1.245	1.088	0.967
0.3659	3.077	2.473	2.061	1.707	1.463	1.274	1.116	0.986
0.4115	3.175	2.536	2.120	1.751	1.496	1.301	1.142	1.004
0.4580	3.252	2.604	2.183	1.789	1.527	1.321	1.156	1.022
η/mPa·s of [C_1C_8IM][OAc] + DMF								
0.0493	1.017	0.902	0.775	0.728	0.662	0.608	0.558	0.517
0.0919	1.046	0.926	0.798	0.745	0.677	0.620	0.570	0.526
0.1364	1.073	0.951	0.817	0.760	0.691	0.634	0.582	0.536
0.1851	1.109	0.978	0.846	0.782	0.705	0.649	0.594	0.548
0.2272	1.131	1.000	0.863	0.796	0.720	0.659	0.603	0.557
0.2776	1.167	1.026	0.889	0.816	0.737	0.671	0.615	0.566
0.3171	1.189	1.040	0.901	0.822	0.747	0.677	0.622	0.571
0.3669	1.214	1.059	0.916	0.835	0.754	0.684	0.625	0.573
0.4086	1.241	1.080	0.930	0.844	0.763	0.691	0.630	0.576
0.4578	1.275	1.100	0.948	0.855	0.768	0.693	0.629	0.574
η/mPa·s of [C_1C_8IM][OAc] + EG								
0.0496	21.235	14.049	9.922	7.041	5.276	4.098	3.260	2.630
0.0975	21.250	14.064	9.945	7.063	5.298	4.118	3.292	2.651
0.1366	21.265	14.075	9.962	7.081	5.312	4.135	3.312	2.666
0.1841	21.282	14.090	9.979	7.108	5.326	4.152	3.340	2.684
0.2313	21.296	14.106	10.001	7.137	5.340	4.172	3.367	2.700
0.2755	21.310	14.125	10.020	7.165	5.352	4.194	3.391	2.714
0.3198	21.327	14.137	10.039	7.192	5.366	4.212	3.416	2.728
0.3698	21.341	14.159	10.065	7.219	5.380	4.237	3.439	2.744
0.4079	21.351	14.174	10.087	7.242	5.391	4.252	3.455	2.756
0.4561	21.362	14.192	10.113	7.267	5.407	4.272	3.476	2.771

Standard uncertainties are $u(m) = 5 \times 10^{-3}$ mol·kg^{-1}, $u(\eta) = 1\%$, $u(P) = 2$ kPa and $u(T) = 0.02$ K.

supported to understand the solute-solvent interactions are more predominate than solute-solute or solvent-solvent interactions. Similar trends were observed for 1-ethyl-3-methylimidazolium methyl sulfate, 1-hexyl-3-methylimidazolium methyl sulfate, 1-hexyl-3-methylimidazolium ethyl sulfate and 1-propyl-3-methylimidazolium bromide with various solvents [30,31].

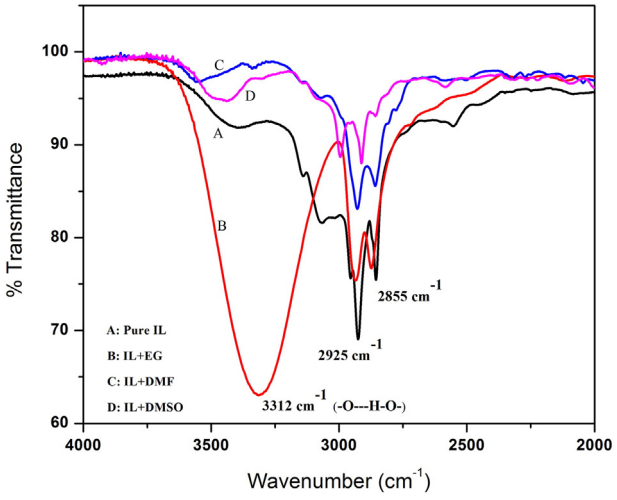

Fig. 5. Normalized FT-IR spectra of pure IL and their binary mixture over the range (4000 to 2000) cm^{-1}.

On the other hand, the apparent molar volume at infinity dilution V_Φ^∞ can be expressed in terms of sum of three contributions such as intrinsic, electrostatic and structural effect as follows

$$V_\Phi^\infty = V_{\text{int}}^\infty + V_{elec}^\infty + V_{str}^\infty \tag{4}$$

The solution volume decreases due to electrostatic force between ions of IL and surrounding molecular solvent molecules. The electrostriction volume is the most significant factor controlling the volumetric properties of smaller cations while the structural contribution is determining the partial molar volume of larger cations. So, the results of apparent molar volumes at infinite dilution of ionic liquid with molecular solvents determined by three contributions such as intrinsic volume, electrostriction volume and structural contribution of the volume [32].

The temperature dependent limiting apparent molar volumes were fitted to second order polynomial equations given as follows

$$V_\Phi^\infty = A + BT + CT^2 \tag{5}$$

where 'A', 'B' and 'C' are empirical constants and 'T' is experimental temperature in Kelvin, the calculated V_Φ^∞ data were reported in Table S1.

The temperature dependent limiting apparent molar expansibility E_Φ^∞ can be calculated by the differentiating Eq. (5) at a constant pressure as given as

$$E_\Phi^\infty = \left(\frac{\partial V_\Phi^\infty}{\partial T}\right)_P = B + 2CT \tag{6}$$

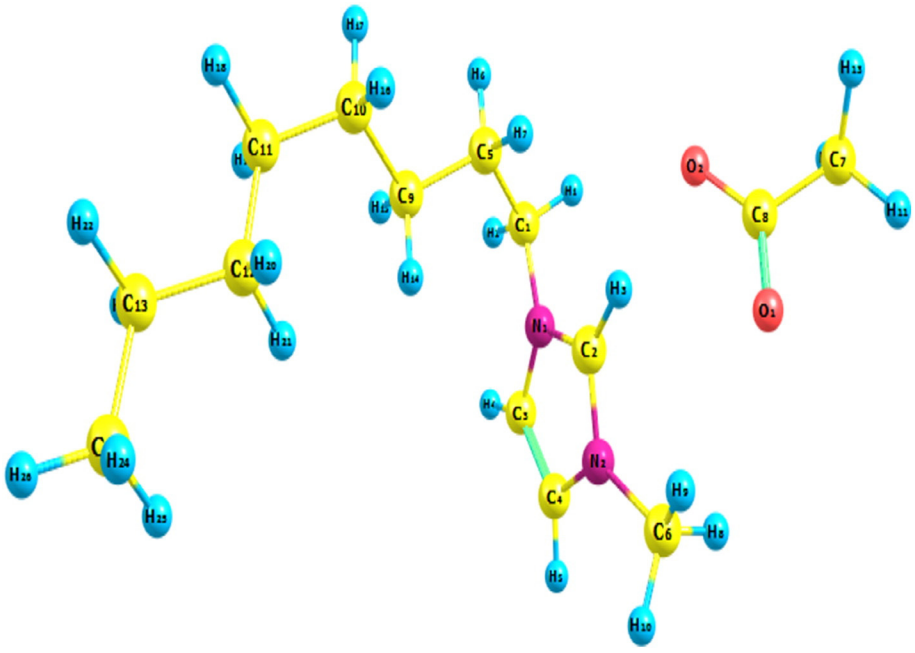

Fig. 6. Geometrical optimized structures of pure [C_1C_8IM][OAc] by using B3LYP/6-311++G (d, p).

The resultant E_{Φ}^{∞} data is summarized in Table S1, the effect of temperature on limiting apparent molar expansibility is graphically illustrated in Fig. 4. A review of Table S1, E_{Φ}^{∞}…data for all systems at each temperature are positive, this suggests that on heating some solvent molecules may be released from the loss of solvation layer of the ions. In addition, it slightly increases with increases in temperature because of the solutions that contains solute molecule (IL ions), which are expanding more rapidly than solvent molecules [33,34].

4.2. Transport properties

Experimentally measured viscosity of pure IL and molecular solvents were listed in Table 1, the viscosity of binary mixtures as a concentration of IL with studied solvents were reported in Table 4 in the temperature range of T = (293.15–363.15) K. From Table 4, it is clear that the viscosity of the binary solution linearly increased with increases of IL concentration, the effect of IL concentration on experimental viscosity is graphically represented in Figs. S7–S9. This is due to the fact that with increases in amount of IL, the mobility of solvent molecules decreases and the resistance between molecules increases [35]. The measured viscosity data of the binary solutions were fitted to Jones-Dole empirical equation [36] to obtain the viscosity B-coefficient, given as follows

$$\eta_r = \frac{\eta}{\eta_o} = 1 + AC^{\frac{1}{2}} + BC \tag{7}$$

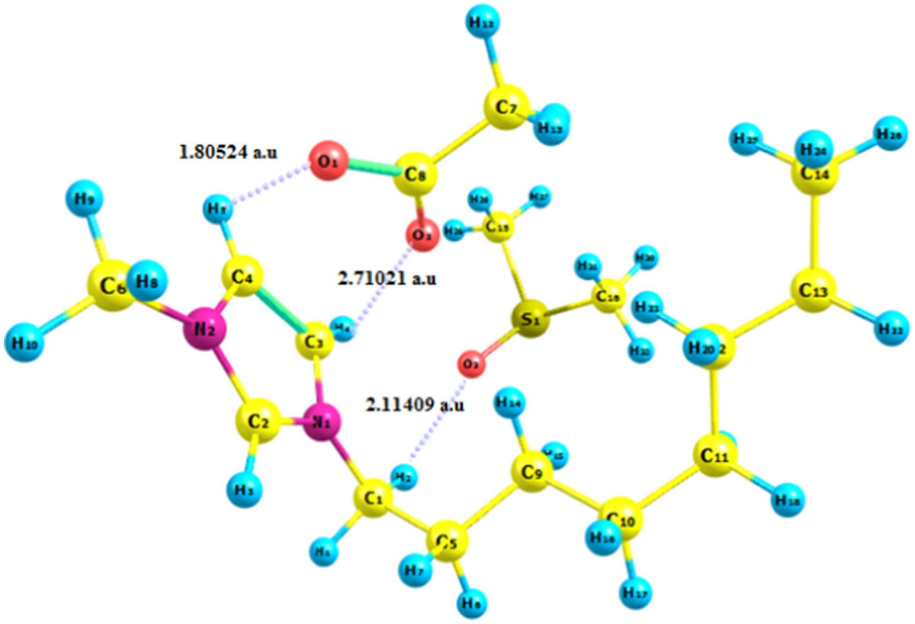

Fig. 7. Geometrical optimized structures of binary mixture of [C_1C_8IM][OAc] + DMSO by using B3LYP/6-311++G (d, p).

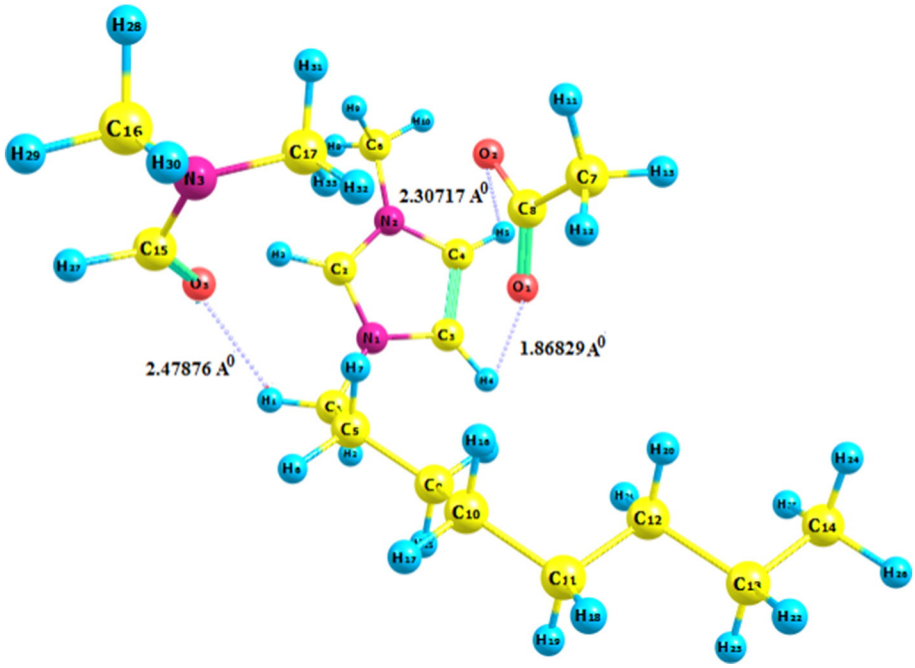

Fig. 8. Geometrical optimized structures of binary mixture of $[C_1C_8IM][OAc]$ + DMF by using B3LYP/63-11++G (d, p).

where η_r is relative viscosity of the solutions, η and η_o are the viscosity of solution and solvents respectively, *C* is concentration of the IL, '*A*' and '*B*' are the coefficients. The resultant coefficients and their ARD values were listed in Table S1, an estimated relative viscosity for all systems at all temperature ranges were given in Table S2. The relative viscosity of the studied binary systems increased with increases the molality of the IL. From Eq. (7) A-coefficient data measures the ion-ion interactions, B-coefficient reflects the effect of solute-solvent interactions on the solution viscosity [37]. The viscosity B-coefficient is provided the valuable information about the solvation of the solutes and their effects on the structure of the solvent in the nearest environment of the solute molecules. The larger and positive B values indicate a structure to allow the solute to act on solvents [38]. In the present investigation an important observation is about the magnitude and temperature variations of the viscosity B-coefficient of IL with molecular solvents. From Table S1 it is observed that a low viscosity B-coefficient for the ILs decreases with increases the temperature, this suggested that presence of strong solute-solvent interactions, this kind of interactions become stronger with increases an ionic liquid concentration.

4.3. FT-IR spectroscopic analysis

FT-IR spectroscopy can be useful to determine the solute-solvent interactions. It has been extensively used to study the intra and intermolecular hydrogen bonding between component molecules. In general, the broad band can observed for the intermolecular hydrogen bonding while the sharp band indicates for an intramolecular hydrogen bonding. In the case of aliphatic pure alcohols, the broad band appeared about at 3400 cm^{-1} which is due to free -OH group in alcohols [39,40]. For alcohols -OH stretching absorption intensity decreases with the increases in concentration of the solute molecules. We could notice clearly that the significant shifts are caused by the strong intermolecular interactions like hydrogen bonding between the oxygen atom directly attached to the carboxylate group and hydrogen of alcohol.

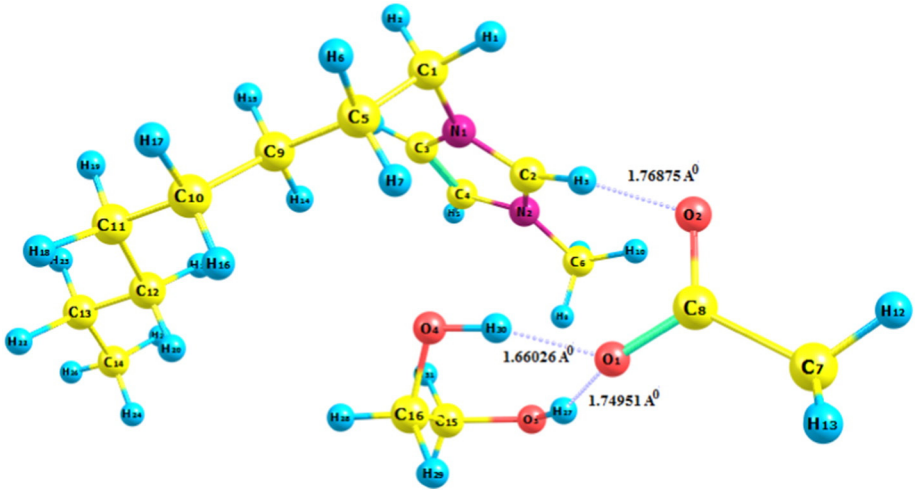

Fig. 9. Geometrical optimized structures of binary mixture of $[C_1C_8IM][OAc]$ + EG by using B3LYP/6-311++G (d, p).

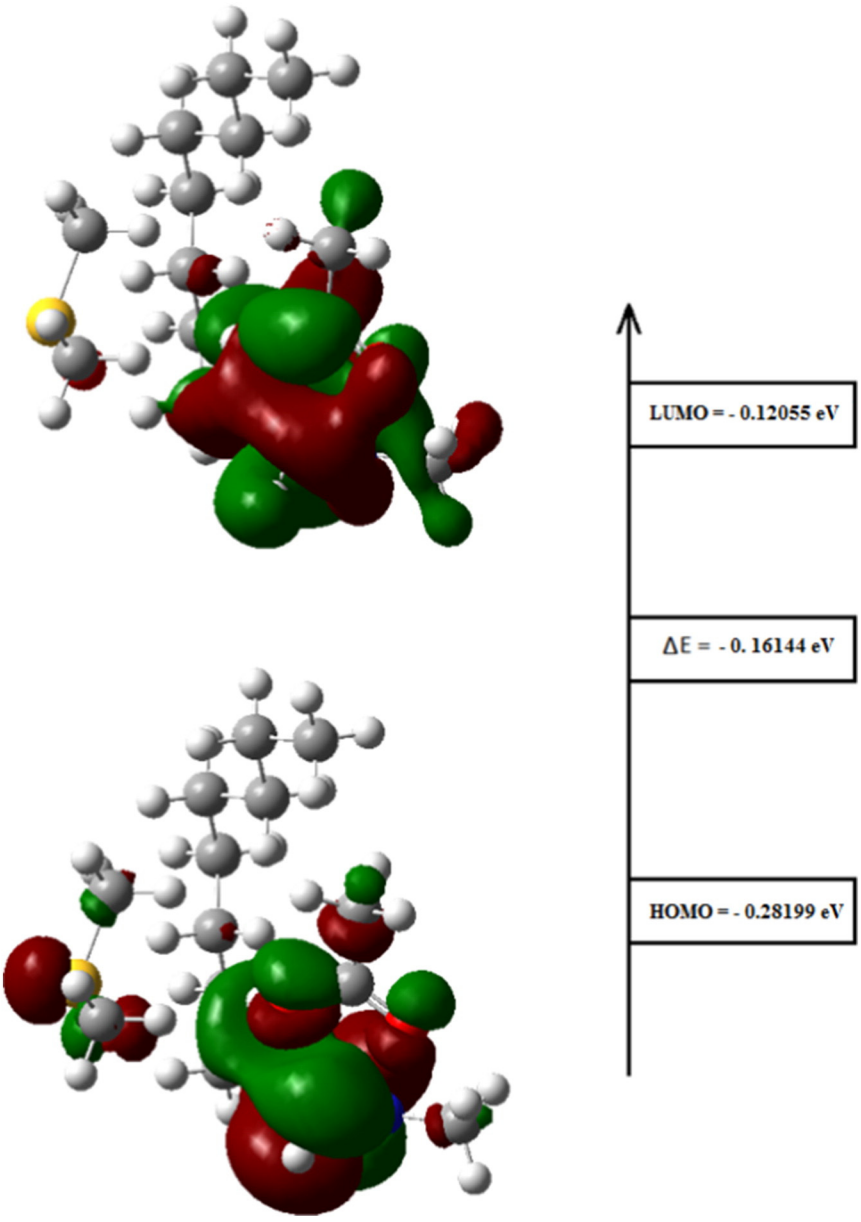

Fig. 10. The HOMO and LUMO study of $[C_1C_8IM][OAc]$ + DMSO.

In the present study FT-IR analysis performed for the binary solutions of IL with molecular solvents such as dimethyl sulfoxide (DMSO), dimethylformamide (DMF) and ethylene glycol (EG) at about m = 0.45 mol·kg^{-1}, at room temperature was shown in Fig. 5. From Fig. 5, high intensity broad band were observed at 3312 cm^{-1} for IL with ethylene glycol solution. This contention was supported by the formation of intermolecular hydrogen bonding (C-O-H-O) between component molecules.

To understand the effect of water content on studied properties of IL, we have measured the density, and viscosity of $[C_1C_8IM][OAc]$ having different water content (574, 2514, 4654and 6694) ppm at 293.15 K. An increase in water content from 574 ppm (dried IL) to 6694 ppm about 0.4% and 1.2% increment is observed in density and viscosity, respectively. Considering the water content present in IL as an impurity, and by extrapolating (the experimental data of densities and viscosity as a function of water content) to zero water content (*i.e.*, for pure ionic liquid). The measured experimental data and the graphical representation given in supporting information file as Table S3 and Fig. S11 respectively.

4.4. Density functional theory study

Density functional theory (DFT) calculations were carried out to understand the structural variations on the intra-ionic and inter-ionic interactions between the cation and anion of the IL and molecular solvents. The Perdew-Wang hybrid (B3PW91) exchange-correlation function with the 6-311G++ (d,p) basis set was used to perform the conformational analysis and geometry optimizations of studied molecules [41]. First, the cation and anion structures are separately optimized and then ion-paired structures *i.e.* combination of cation and anion to simulate the complete IL, the geometrical representation of complete structures of IL is given as Fig. 6. The optimized structures with electrostatic potential (ESP) mapped on to an electronic density surfaces and are calculated by B3LYP/6–

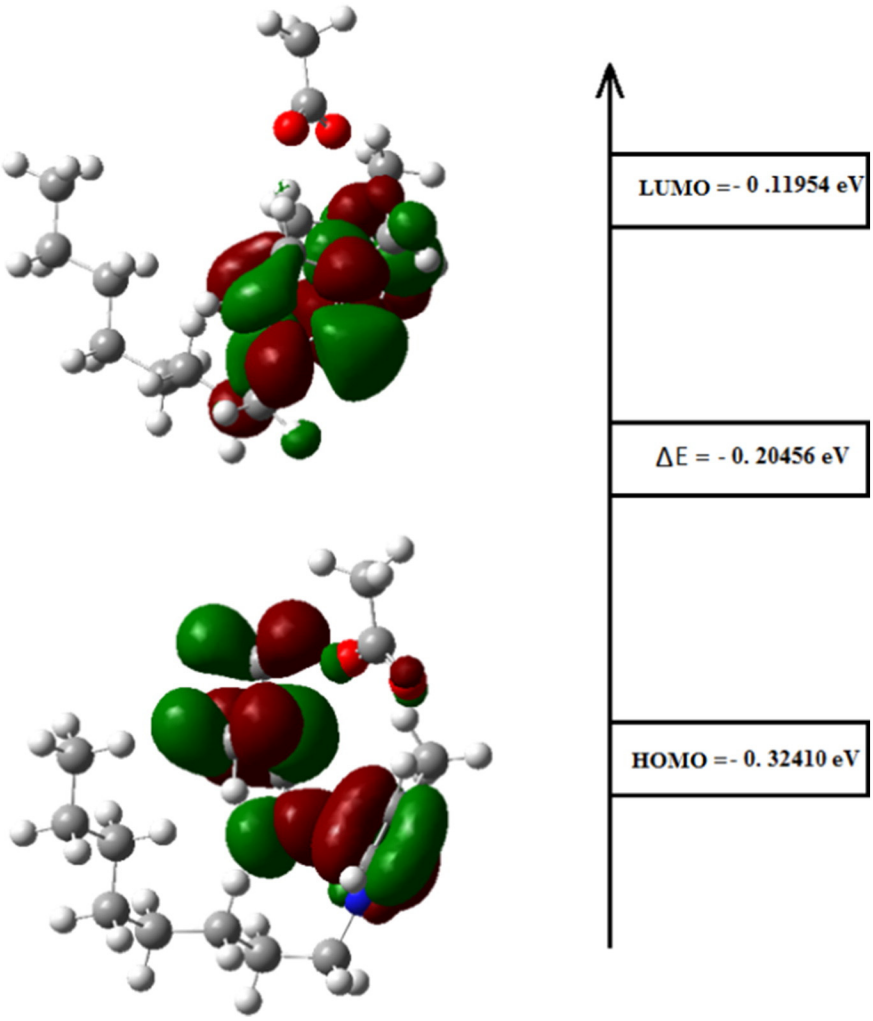

Fig. 11. The HOMO and LUMO study of $[C_1C_8IM][OAc]$ + DMF.

311++g (d,p) theoretical level for $[C_1C_8IM][OAc]$, DMSO, DMF and EG molecules which are represented in Fig. S10. In addition, the binding energies for isolated IL with molecular solvents were performed with the basis set superposition error (BSSE) using the Boys Bernardi counterpoise technique [42]. From Figs. 7–9 the capability of formation of inter-ionic and intra-ionic molecular interactions and hydrogen bonding could be seen. To understand the H-bonding of IL with studied molecular solvents, the possible H-bonding interactions (Fig. 9) C_8-O_1-H_{27}-O_3 (Å = 1.75 a.u), and C_8-O_1-H_{30}-O_4 (Å = 1.66 a.u) were observed. Patricia et al., have clearly explained that the bond distance about 1.5–2.2 Å required to the formation of H-hydrogen bonding between the inter molecules [43] (electronegative atom and hydrogen atom), this contention also have supported to present investigation. Moreover, the natural bond orbital (NBO) data is a reliable tool for the rationalization of H-bonds that correlate and changes in bond length between component molecules. An interaction energy (ΔE) for the binary mixtures of hydrogen bonded complexes and the summation of the energy of the component molecules given as follows

$$\Delta E = E_{complex} - \sum E_{components}$$

This also provides valuable information about the changes of charge densities of proton donor and acceptor as well as in the bonding and antibonding orbitals. The HOMO and LUMO analyses can give insight into the chelating process of solute-solvent systems. LUMO is associated with the tendency of a species to receive electron and is characteristic for electrophilic components, while HOMO is associated with the tendency to donate electron and is characteristic for nucleophilic components [44]. Thus, the HOMO and LUMO are a likely location for a bond to occur between the solute and solvent because the incoming electron from HOMO of one molecule will fill into the LUMO of another molecule. The HOMO and LUMO of studied IL with molecular solvents, their energy levels and energy variations are illustrated as Figs. 10–12, this figures explained that the energy gap (ΔE) between HOMO and LUMO are −0.211 eV, −0.205 eV and −0.161 eV for IL + EG, IL + DMF and IL + DMSO respectively, IL + EG showed the lowest energy difference and it may give strong interactions when compare to other systems. An interaction energy corrected with basis set superposition error (BSSE) (ΔE_{cp}·kcal·mol^{-1}) for all systems are listed in Table 5.

5. Conclusions

In the present study 1-octyl-3-methylimidazolium acetate ionic liquid was synthesized and characterized by ^{1}H and ^{13}C NMR spectroscopy. Density and viscosity of the pure components such as $[C_1C_8IM][OAc]$, DMSO, DMF and EG have been measured in the temperature range of T = (293.15–363.15)K at 0.1 MPa pressure. The volumetric and transport properties have also been measured for the binary solutions of IL with molecular solvents as a function of IL concentration (m, 0.0451–0.4960 mol·kg^{-1}). The measured density data could be

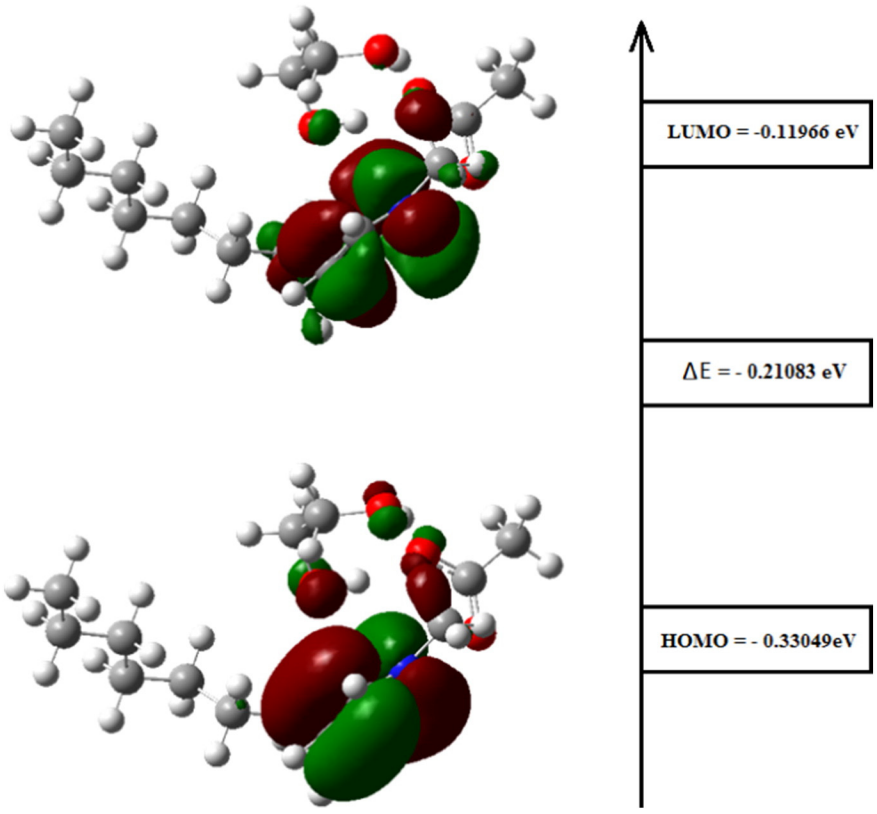

Fig. 12. The HOMO and LUMO study of [C_1C_8IM][OAc] + EG.

Table 5
Interaction energy corrected with BSSE (ΔE_{cp}·kcal·mol^{-1}) for all dimmers at B3LYP/6-311++G (d,p) level.

Complexes	ΔE	BSSE	ΔE_{cp}
IL + DMSO	−1.89	0.11	−1.79
IL + DMF	−2.36	0.21	−2.15
IL + Eg	−3.59	0.26	−3.33

The standard uncertainties are $u(\Delta E) = 0.02$ eV, u(BSSE) = 0.05 (ΔE_{cp}·kcal·mol^{-1}), $u(\Delta E_{cp}) = 0.05$ eV.

useful to calculate the apparent molar volume, apparent molar volume at infinity dilutions and apparent molar volume expansibility by using the Redlich-Mayer equation. The results could be concluded that the solute-solvent interactions are more predominate than compare to solute-solute or solvent-solvent interactions. Jones-Dole empirical equation could be help full to determine the B-coefficient through the relative viscosity calculations, which was determined from measured viscosity data of binary systems at all temperature and concentration ranges. The positive and low B-coefficient data seems to be the solvation of the solutes and their effects on the structure of the solvent in the nearest environment of the solute molecules. In addition, FT-IR spectroscopy technique and density functional theory (DFT) also were performed to conform the solute-solvent interactions, IL + EG showed stronger interactions (H-bonding) than compared to other ionic solutions.

Acknowledgments

Authors would like to acknowledge to the Center of Research in Ionic Liquids (CORIL), Universiti Teknologi PETRONAS, Perak, Malaysia and Department of Physics, Vignan Institute of Technology and Science, Deshmukhi, Telangana, India respectively, for the financial support.

Appendix A. Supplementary data

Supplementary data to this article can be found online at http://dx.doi.org/10.1016/j.molliq.2016.10.046.

References

[1] V. Losetty, B.K. Chennuri, R.L. Gardas, J. Chem. Thermodyn. 90 (2015) 251–258.
[2] J. Dupont, R.F. De Souza, P.A.Z. Suarez, Chem. Rev. 102 (2002) 3667–3692.
[3] J.L. Anthony, E.J. Maginn, J.F. Brennecke, J. Phys. Chem. B 105 (2001) 10942–10949.
[4] M. Xiao-Xue, W. Jie, Z. Qiu-Bo, T. Fang, F. Ying-Ying, G. Wei, Ind. Eng. Chem. Res. 52 (2013) 9490–9496.
[5] H.F.D. Almeida, H. Passos, J.A. Lopes-da-Silva, A.M. Fernandes, M.G. Freire, J.A.P. Coutinho, J. Chem. Eng. Data 57 (2012) 3005–3013.
[6] B.K. Chennuri, V. Losetty, R.L. Gardas, J. Mol. Liq. 212 (2015) 444–450.
[7] J. Wang, H. Jiang, Y. Liu, Y. Hua, J. Chem. Thermodyn. 43 (2011) 800–804.
[8] T. Zamir, T.I. Quickenden, J. Solut. Chem. 32 (2003) 463–472.
[9] A. Huang, C. Liu, L. Ma, Z. Tong, R. Lin, J. Chem. Thermodyn. 49 (2012) 95–103.
[10] A.A. Mohammad, K.H.A.E. Alkhaldi, M.S. AlTuwaim, A.S. Al-Jimaz, J. Chem. Thermodyn. 56 (2013) 106–113.
[11] G.H. Min, Y. Taeeun, H. Yeong Lee, D.H. Huh, E. Lee, J. Mun, S.M. Oh, Y.G. Kim, Bull. Kor. Chem. Soc. 27 (2006) 847–852.
[12] V.D. Sergei, D.K. Katherine, S.S. Salil, J. Chem. Educ. 86 (2009) 856–858.
[13] O. Iulian, O. Ciocirlan, J. Chem. Eng. Data 57 (2012) 2640–2646.
[14] O. Ciocirlan, O. Iulian, J. Chem. Eng. Data 57 (2012) 3142–3148.
[15] X. Wang, F. Yang, Y. Gao, Z. Liu, J. Chem. Thermodyn. 57 (2013) 145–151.
[16] C. Yang, G. He, Y. He, P. Ma, J. Chem. Eng. Data 53 (2008) 1639–1642.
[17] C. Yang, G. Wei, Y. Li, J. Chem. Eng. Data 53 (2008) 1211–1215.
[18] J.M. Bernal-Garcia, A. Guzman-Lopez, A. Cabrales-Torres, A. Estrada-Baltazar, G.A. Iglesias-Silva, J. Chem. Eng. Data 53 (2008) 1024–1027.
[19] G.T. Nikos, E.K. Antonis, M.P. Maria, J. Chem. Eng. Data 45 (2000) 395–398.
[20] F. Comelli, R. Francesconi, A. Bigi, K. Rubini, J. Chem. Eng. Data 52 (2007) 639–644.
[21] C. Yang, P. Ma, F. Jing, D. Tang, J. Chem. Eng. Data 48 (2003) 836–840.
[22] C. Yang, Z. Liu, H. Lai, P. Ma, J. Chem. Eng. Data 51 (2006) 457–461.
[23] A.B. Bilkis, S.K. Biswas, M. Alamgir, Indian J. Chem. 15 (1996) 127–132.
[24] A.D. Becke, Phys. Rev. A 38 (1988) 3098–3100.
[25] M. Raveendra, M. Chandrasekhar, C. Narasimha Rao, L. Venkatramanna, K. Siva Kumar, K. Dayananda Reddy, RSC Adv. 6 (2016) 27335–27348.
[26] D. Keshapoll, V. Singh, R.L. Gardas, J. Mol. Liq. 199 (2014) 330–338.
[27] O. Redlich, D.M. Meyer, Chem. Rev. 64 (1964) 221–227.
[28] J. Ananthaswamy, G. Atkinson, J. Chem. Eng. Data 29 (1984) 81–87.

[29] Y. Li, E.J.P. Figueiredo, M. Santos, J. Santos, N.M.C. Talavera-Prieto, P.J. Carvalho, A.G.M. Ferreira, S. Mattedi, J. Chem. Thermodyn. 88 (2015) 44–60.
[30] H. Shekaari, E. Armanfar, Fluid Phase Equilib. 303 (2011) 120–125.
[31] R. Sadeghi, H. Shekaari, R. Hosseini, Int. J. Thermophys. 30 (2009) 1491–1509.
[32] L. Marcinkowski, T. Olszewska, A. Kloskowski, D. Warminska, J. Chem. Eng. Data 59 (2014) 718–725.
[33] M.T. Zafarani-Moattar, H. Shekaari, J. Chem. Thermodyn. 37 (2005) 1029–1035.
[34] O. Popovych, R.P.T. Tomkins, Non-Aqueous Solution Chemistry, John Willey & Sons, Inc., New York, 1981.
[35] S. Hemayat, K. Amir, Fluid Phase Equilib. 309 (2011) 1–7.
[36] G. Jones, M. Dole, J. Am. Chem. Soc. 51 (1929) 2950–2964.
[37] C. Zhao, P. Ma, J. Li, J. Chem. Thermodyn. 37 (2005) 37–42.
[38] R.H. Stocks, R. Milles, Interactional Encyclopedia of Physical Chemistry and Chemical Physics, Pergamon, New York, 1965.
[39] R.M. Silverstein, G.C. Bassler, T.C. Morrik, Spectroscopic Identification of Organic Compounds, fourth ed. John Wiley & sons, Inc., Singapore, 1991.
[40] L. Venkatramana, C. Narasimha Rao, K. Sivakumar, R.L. Gardas, J. Mol. Liq. 209 (2015) 578–585.
[41] Y. Zhao, J. Wang, H. Wang, Z. Li, X. Liu, S. Zhang, J. Phys. Chem. B 119 (2015) 6686–6695.
[42] M. Anouti, J. Jacquemin, P. Porion, J. Phys. Chem. B 116 (2012) 4228–4238.
[43] A.H. Patricia, R.A. Claire, P.M. Richard, Chem. Soc. Rev. 44 (2015) 1257–1288.
[44] R. Shahid, N. Muhammad, G. Gonfa, M.S. Toprak, M. Muhammed, J. Phys. Chem. Solids 85 (2015) 34–38.